Isolation of a novel Pythium mosquito larval pathogen, P. themoculicivorax, and Trichoderma sp. from natural enzootic mosquito larval infections

Ross Joseph , Constance Darrisaw , Aaron Lloyd , David F. Hoel * , Nemat Oliver Keyhani *

Posted Date: 28 February 2024

doi: 10.20944/preprints202402.1594.v1

Keywords: oomycete, Pythium, mosquito larvae, thermotolerance, microbial pathogen, Trichoderma

Article

Isolation of a Novel *Pythium* Species, *P. themoculicivorax*, and *Trichoderma* sp. from Natural Enzootic Mosquito Larval Infections

Ross Joseph [1], Constance Darrisaw [2], Aaron Lloyd [2], David Hoel [2,*] and Nemat O. Keyhani [1,*]

[1] Department of Biological Sciences, University of Illinois, Chicago, IL, 60607; rossj@uic.edu
[2] Lee County Mosquito Control District, Lehigh Acres, FL 33971; CD: darrisaw@lcmcd.org; AL: lloyd@lcmcd.org
* Correspondence: hoel@lcmcd.org (D.L.); keyani@uic.edu (N.O.K.)

Abstract: Only a handful of microbial mosquito larval pathogens have been described to date. Sampling of several natural enzootic infections of mosquito larvae in southwestern Florida indicated the presence of microbial pathogens capable of extensive larval mortality. Microscopic analysis of one sample site revealed extensive apparent growth of a *Pythium*-like microbe on mosquito larvae, with highest infection observed on the siphon and head regions. Structures consistent with sporangia were seen on infected insects after lactophenol blue staining, and higher resolution scanning electron micrographs (SEM) showed sporangia and encysted zoospores targeting the head and siphon regions. The isolate was single colony purified and molecular identification targeting the ITS and COX1 loci coupled to phylogenetic reconstruction indicated that the isolate belonged to the *Pythium* genus, but was distinct from its closest characterized species, *P. inflatum*. Morphological features were characterized, with the isolate showing rapid growth on all mycological media tested and relatively high thermotolerance, capable of robust growth at 37°C, and hence was designated, *P. thermoculicivorax*. Sampling from a second series of natural infections of mosquito larvae resulted in the molecular identification of three *Trichoderma* isolates, one with high similarity to *T. strigosum*, and the other two clustering closely with *T. asperellum*. These data highlight the occurrence of natural enzootic infections of mosquito larvae, potentially as a resource for the identification of new mosquito pathogens.

Keywords: oomycete; *Pythium*; mosquito larvae; thermotolerance; microbial pathogen; *Trichoderma*

1. Introduction

Interest in microbial insect pathogens stems, in part, as biological agents that can be used as alternatives to chemical pesticides due to their lower environmental toxicity and decreased off-target effects [1–3]. Examining naturally occurring enzootic diseases, particularly of insect pests, is important for increasing our understanding of basic ecological processes, but also represents a reservoir for the discovery of locally adapted biological agents that could potentially be exploited for pest control [4–6]. Mosquitoes represent a major global health threat due to the variety of disease-causing agents, ranging from viruses (e.g., dengue, yellow fever, Zika), and parasites (e.g., malaria-causing *Plasmodium* sp.), that they vector [7–9]. Human and animal (livestock) cases exceed hundreds of millions per year, resulting in significant social and economic losses, with several million deaths of human and livestock animals reported annually, and even links to certain cancers suspected [10,11]. Both biological and chemical methods have been used to control mosquito populations, with the latter predominating, however, development of resistant populations to synthetic chemical pesticides and increasing regulatory burdens have shifted some attention to the former category [12–15]. Amongst the microbial biological agents, the best characterized are members of the Ascomycete entomopathogens (e.g., *Beauveria* and *Metarhizium* sp.), some of which have been commercialized for the control of larvae and adults of a range of mosquito species including those that have developed resistance to chemical pesticides [16–21]. In addition, several mosquito pathogens within the

 doi:10.20944/preprints202402.1594.v1

Oomycota, which represent a distinct phylogenetic lineage (pseudofungi, Stramenopiles) apart from the Fungal Kingdom, include a variety of plant and animal pathogens previously described [22–24].

Of oomycete mosquito pathogens, *Lagenidium giganteum* (Couch ex Redhead, 2015) has been widely examined as a potential mosquito larval pathogen, with a commercialized product briefly approved by the US Environmental Protection agency [25–28]. The product was subsequently deregistered due to the reporting of several cases of *L. giganteum* mediated near-fatal infections in dogs in the southern US. Two populations of *L. giganteum* have been reported, and while both are able to infect mosquito larvae, one, labeled as heat tolerant (capable of growing at 37°C), appears to infect mammals, and the other, heat-sensitive (incapable of growing at 37°C), infects mosquito larvae in nature [28,29]. Characterization of additional isolates from fly, mosquito, and a dog with lagenidiosis (the former two heat-sensitive, the latter heat-tolerant) identified a new species named *L. juracya* (Vilela, Humber, Taylor, and Mend, 2019), and the dog derived isolate as *Paralegenidium ajellopsis* (Vilela, Humber, Taylor and Mend, 2019) [24]. *Leptolegnia chapmanii* (Seym, 1984) is another oomycete pathogen of mosquito larvae, with various life cycle parameters and histological examination of zoospore penetration via the integument and gut described [23,30,31]. More recently, *L. chapmanii* has been shown to be compatible with the chemical insecticide diflubenzuron and with neem oil, potentially as part of an integrated pest management (IPM) strategy for larval mosquito control [32].

Several *Pythium* species have also been described as mosquito pathogens including *P. carolinianum* (Matthews, 1931), *P. guiyangense* (Su, 2006), and even isolates of the mammalian pathogen, *P. insidiosum* (De Cock, Mend, Padhye, Ajello and Kaufman, 1987) [33–35]. Genomic sequencing and molecular studies have identified aspects of the infection mechanism and annotated a set of effector proteins in *P. guiyangense* [36,37], although these studies lag far behind those on plant pathogenic oomycetes. Here, we report on the occurrence of several natural enzootic infections of mosquito larvae in the southwestern part of Florida. Microscopic, physiological, and sequencing and analyses of marker genomic loci (ITS and COXI) indicated the identification of a new, heat tolerant *Pythium* species, designated *P. thermoculicivorax*, while sequencing of markers ITS, RPB2, and TEF1a revealed three mosquito pathogenic *Trichoderma* isolates, one of which partitioned with *T. strigosum* (Bissett, 1991), whereas the other two were closely related to each other and clustered with *T. asperellum* (Lieckfeldt and Nirenberg, 1999).

2. Materials and Methods

Collecting mosquito larvae

Larval collection was completed using a standard larval dipper (Clarke St. Charles, IL, USA) and a fine mesh food strainer (AIYoo, Amazon.com) functioning as a hand sieve. When a potential larval breeding site was found, the dipper was used to scoop a visible group of larvae or debris where larvae may have been hiding. The contents of the dipper were poured through the hand sieve to remove excess water. Sieved larvae were rinsed with source water into a collection container. Once enough larvae were collected, a small amount of water from the larval source was added to the container to ensure larval survival during transport. Once brought into the insectary, larvae were sieved again to separate by size and remove debris. They were rinsed with clean water and added to pans of filtered tap water. Subsets of each collected larval sample were separated and taken to the microscope to determine the presence and degree of pathogen infection. All mosquito larvae were identified by eye, then confirmed under a microscope using Darsie and Ward [38]. For most samples, a record was kept of the mosquito species, the location of collection, the larval instar, and the degree of infection, if any, at the time of reception.

Isolation of Pythium and Trichoderma strains

Infected mosquito larvae collected in Lee County were sealed in plastic bags half-filled with water and shipped on ice overnight to the University of Florida (main campus, Gainesville, Florida) for isolation of *Pythium* and *Trichoderma* species. Upon receipt, larvae were removed from the bag

 doi:10.20944/preprints202402.1594.v1

and placed into a petri dish filled with sterile distilled water. To wash the larvae, the dish was swirled and then the water removed and replaced with fresh sterile distilled water. A total of three washes were performed in this manner. Individual larvae were plated on 60mm PDA plates amended with 200µg/mL ampicillin and streptomycin by cutting a small wedge out of the agar in the center of the plate and placing the larvae inside. Plates were incubated at room temperature (~24°C) and examined daily under a dissecting microscope. Hyphae observed emerging from larval bodies and growing into agar were excised with a sterile razor blade and plated onto a fresh plate with selection as before. Isolates were purified three times by hyphal tipping and were then maintained at room temperature on PDA.

Pythium temperature growth tolerance assays

To test the extent of growth of *Pythium* cultures at varying temperatures, agar wedges containing hyphae at the edges of actively growing cultures were cut from a PDA culture and used to inoculate the center of fresh PDA plates. In triplicate, plates were incubated at 20°C, 26°C, and 37°C for 4 days. Relative growth was assessed by measuring colony diameter on each plate.

DNA extraction, PCR, Sequencing

To extract DNA from *Pythium* and *Trichoderma* isolates, 100mm PDA plates were overlayed with a cellophane disk, which allowed fungi to access nutrients from the medium, but not to penetrate the agar with their hyphae. Plates were then inoculated on top of this cellophane layer by placing a small wedge of agar containing hyphae of the desired isolate. Plates were allowed to grow at room temperature for 4-7 days, until hyphae had spread to cover the cellophane disk, after which point the hyphae was scraped off the surface of the cellophane and placed into sterile 2ml lock cap tubes containing a single sterile glass bead. Tubes containing tissue were then snap frozen in liquid nitrogen and lyophilized. Lyophilized tissue samples were then lysed in a bead beater (MP Fast-Prep 24, 4.0 m/s for 60 seconds). DNA was extracted from powdered tissue using the Plant/Fungi DNA Isolation Kit (Norgen Biotek, Thorold, ON, CA) and quality was assessed using a nanophotometer (Implen, model NP80, Westlake Village, CA, USA). Extracted DNA was used as a template to amplify ITS/LSU and COX1 regions from *Pythium* isolate and ITS/LSU, TEF1a, and RPB2 regions from *Trichoderma* isolates using the primer sets UN-up18S42/UN-lo28S1220 (ITS/LSU), OomCoxI-Levup/Fm85mod (COX1), EF1-728F/TEF1LLErev (TEF1), and fRPB2-5F/fRPB2-7cr (RPB2) [39,40]. Taq 5x Master Mix (New England Biolabs, Ipswich, MA, USA) was used for all PCR reactions according to manufacturer instructions and amplification was confirmed by gel electrophoresis. PCR reactions were purified using the GeneJET PCR Purification Kit (Thermo Scientific, Waltham, MA, USA) and sequenced by Sanger sequencing (Pythium COX1, Trichoderma ITS/LSU) or Oxford Nanopore sequencing (Pythium ITS/LSU, Trichoderma TEF1 and RPB2) using the same primers as for PCR by Eton Biosciences (San Diego, CA, USA) and Plasmidsaurus (Eugene, OR, USA), respectively.

Generating Phylogenies

Following sequencing, data was downloaded and manually assessed in Geneious Prime (Biomatters, Inc, Boston, MA, USA) (Geneious Prime 2023.2, https://www.geneious.com). Ends of forward and reverse sequences for Sanger sequenced samples were trimmed with an error probability limit of 0.05 and read directions were set. Sequences were then aligned using Geneious Alignment with alignment type set to global alignment with free end gaps and a 65% similarity (5.0/-4.0) cost matrix, and consensus sequences were generated using highest quality thresholds (60%), assign quality to total, and calling sanger heterozygotes >50%. Consensus DNA sequences were then exported from Geneious Prime and along with previously published barcoding data of each locus for closely related *Pythium* or *Trichoderma* isolates, respectively, were aligned using MAFFT v. 7.520 with default settings (gap opening penalty of 1.53, offset of 0.0, maximum number of iterative refinement 0). Following alignment, sequences were trimmed using Gblocks with a minimum block length set to 5 [41]. Trimmed sequence alignments for each locus were concatenated using the concat function

 doi:10.20944/preprints202402.1594.v1

in the Seqkit program for *Pythium* and *Trichoderma* sequences, respectively, and concatenated alignments were used to construct and test maximum likelihood trees using RAxML [42] with bootstrap values set to 2000 replicates. Trees were visualized in R Studio using the GGtree package [43]. Branch support values above 70 were displayed on trees. For *Trichoderma* TEF1a and RPB2 sequences and Pythium ITS/LSU sequence, PCR samples were sequenced using Oxford Nanopore long read sequencing (Plasmidsaurus, Eugene, OR, USA) and contigs were used directly in downstream sequence alignment and tree generation after assessing sequence quality by BLAST alignment.

Microscopy

To image *Pythium* zoospores bound to the surface of infected mosquito larvae, individual larvae were first placed into empty 60mm petri dishes and washed with sterile distilled water. This water was then removed and several drops of lactophenol cotton blue (Thermo Scientific, Waltham, MA, USA) were applied directly to the larvae and allowed to sit for several minutes before being removed with several more washes of sterile distilled water. Whole stained larvae were then imaged using a Zeiss Stemi 305 dissecting microscope (Zeiss Group International). For higher magnification imaging of *Pythium* hyphae and other morphological structures, small amounts of actively growing cultures were cut out of petri dishes, stained with lactophenol cotton blue, mounted on glass slides, and cover slipped, or actively growing hyphae from *Pythium* cultures were used to inoculate thin layers of PDA poured directly onto glass slides and incubated in a humid Tupperware container overnight before lactophenol blue staining. In both cases, after staining, samples were cover slipped and imaged at either 40x or 100x objective magnification using a Motic BA310E compound microscope with an attached Moticam X3 (Microscope Central, Feasterville, PA, USA) and a Keyence BZ-X800 fluorescence microscope (Keyence, Osaka, Japan) using brightfield settings. For *Trichoderma* microscopy, hyphae and spores were collected from plate cultures using a toothpick and suspended in water. 5-10 µL of this solution was placed on a microscope slide and 5 µL lactophenol blue was added to the drop to stain fungal tissue. Slides were imaged as above using a Keyence BZ-X800 microscope. To obtain scanning electron microscopy images, mosquito larvae were immersed into 4% paraformaldehyde and 2.5% glutaraldehyde in cacodylate buffer overnight at 4°C. The fixed larvae were washed with 0.1 M cacodylate buffer three times, followed by 2% buffered osmium tetroxide. The post-fixed larvae were water-washed and dehydrated in a graded ethanol series of 25% through 100% with increasing concentrations of 5% to 10%. Following ethanol dehydration, the larvae were critical point dried, including overnight stasis mode (Autosamdri-815; Tousimis, Rockville, MD, USA). The dried larvae were mounted on carbon adhesive tabs on aluminum specimen mounts and gold-palladium sputter coated. The specimens were examined by secondary electrons (SE) on a field emission SEM (SU-5000; Hitachi High Technologies America, Schaumburg, IL, USA).

3. Results

Sampling sites, and macroscopic and microscopic characterization of infected mosquitoes.

From late September until early November 2021, significant infection and mortality of mosquito larvae at eight different sites, some of which were sampled twice, within Lee County Florida were noted (Fig. 1, Supplemental Table S1). Infection appeared to be >80%, with infected larvae including species visually identified as *Culex nigripalpus* (Theobald, 1901), *Psorophora columbiae* (Dyar & Knab, 1906), and *Aedes taeniorhynchus* (Wiedemann, 1821). Similarly, from early May until early December 2022, infected mosquito larvae were seen at various sites within Lee County that included the above listed species, as well as infected *Culex interrogator* (Dyar & Knab, 1906) and *Culex quinquefasciatus* (Say, 1823) (Supplemental Table S1). Mosquito larvae were collected from three sites (in 2022), all containing infected *Ps. columbiae* larvae and further characterized as detailed below. Enzootic infections of mosquito larvae corresponding to *Cx. quinquefasciatus*, *Ae. taeniorhynchus*, *Aedes albopictus* (Skuse, 1894), and *Ps. columbiae* were also noted at various Lee County sites in May and September 2023.

 doi:10.20944/preprints202402.1594.v1

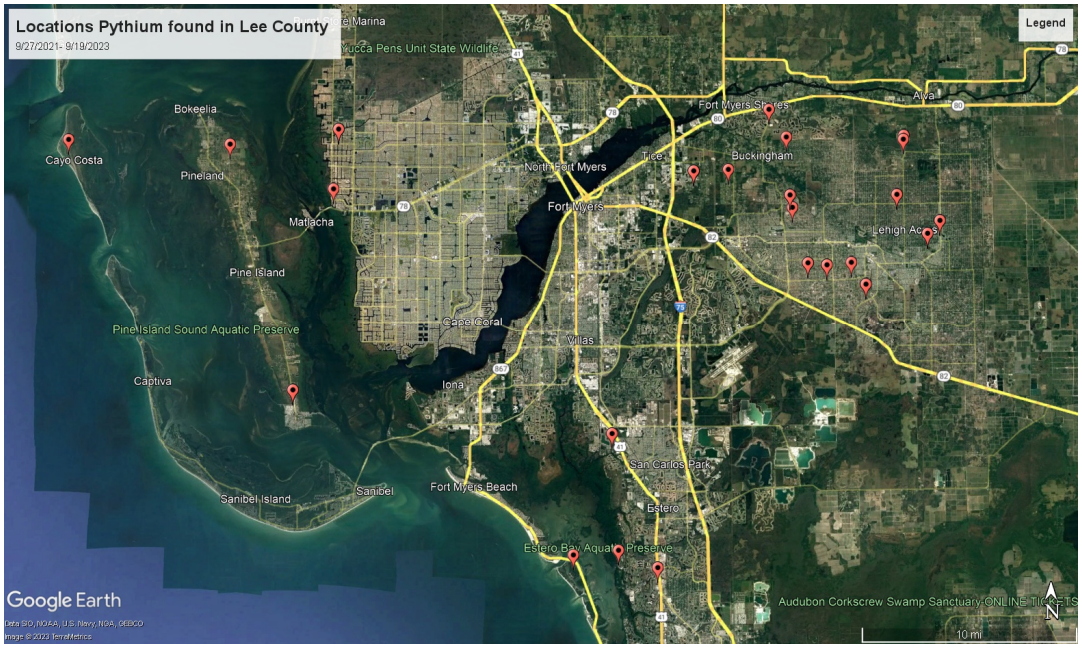

Figure 1. Geolocation map of *Pythium thermoculicivorax* infected larval collections throughout Lee County, FL.

Sample I: collected 8/26/22 (Mercedes Court., Lehigh Acres, FL), mosquito larvae from the sample site were visually inspected with apparent external microbial growth throughout the bodies of most larvae collected (Fig. 2). Clumps of cells could be seen on the head, thorax, and abdomen along various larval segments, as well as on seemingly indiscriminate hairs throughout the body. Compound microscopic visualization indicated that most samples appeared to display similar microbial growth morphology on the larvae (24 examined). To better observe the microbial growth, infected larvae were gently washed and stained with lactophenol blue (Fig. 3). Whole stained mosquito larvae showed clusters of blue stained cells dispersed throughout the body, with higher magnification often showing the strongest staining (and presumed microbial growth) at the head and along the siphon regions, including along the anal segment and pecten, with the latter region often showing the highest levels of infection as seen by the intensity of dye staining (Fig. 3A-C). Higher resolution images of the cells on the larval cuticle revealed round to oval globular cells consistent with oogonia (Fig. 3D & E). Apparent encysted zoospores with infection and attachment structures could also be seen (Fig. 3E & F). In order to provide further morphological details of the infectious cells, infected larvae were processed for scanning electron microscopy (SEM) as detailed in the Methods section. At lower magnification, clumps of encysted zoospores could readily be identified on the mosquito larvae (Fig. 4A & B). Higher resolution imaging revealed slightly oblong encysted zoospores, with attachment and penetration tube-like structures evident (Fig. 4C-E). A distinct pore-like puckered striated opening/structure could be seen at the opposite end of the attachment tubes (Fig. 4F). For isolation, infected larvae were placed into a small divot cut into the center of a PDA plate amended with streptomycin and ampicillin and observed daily under a dissecting scope for the emergence of hyphae from the larval body into the agar. Tips of emerging hyphae were removed with a sterile scalpel blade and inoculated into the center of fresh PDA plates with streptomycin and ampicillin to isolate cultures. This isolated strain was hyphal tipped three successive times onto new PDA with streptomycin and ampicillin plates to obtain a pure culture, resulting in isolate LCMP-P1.

 doi:10.20944/preprints202402.1594.v1

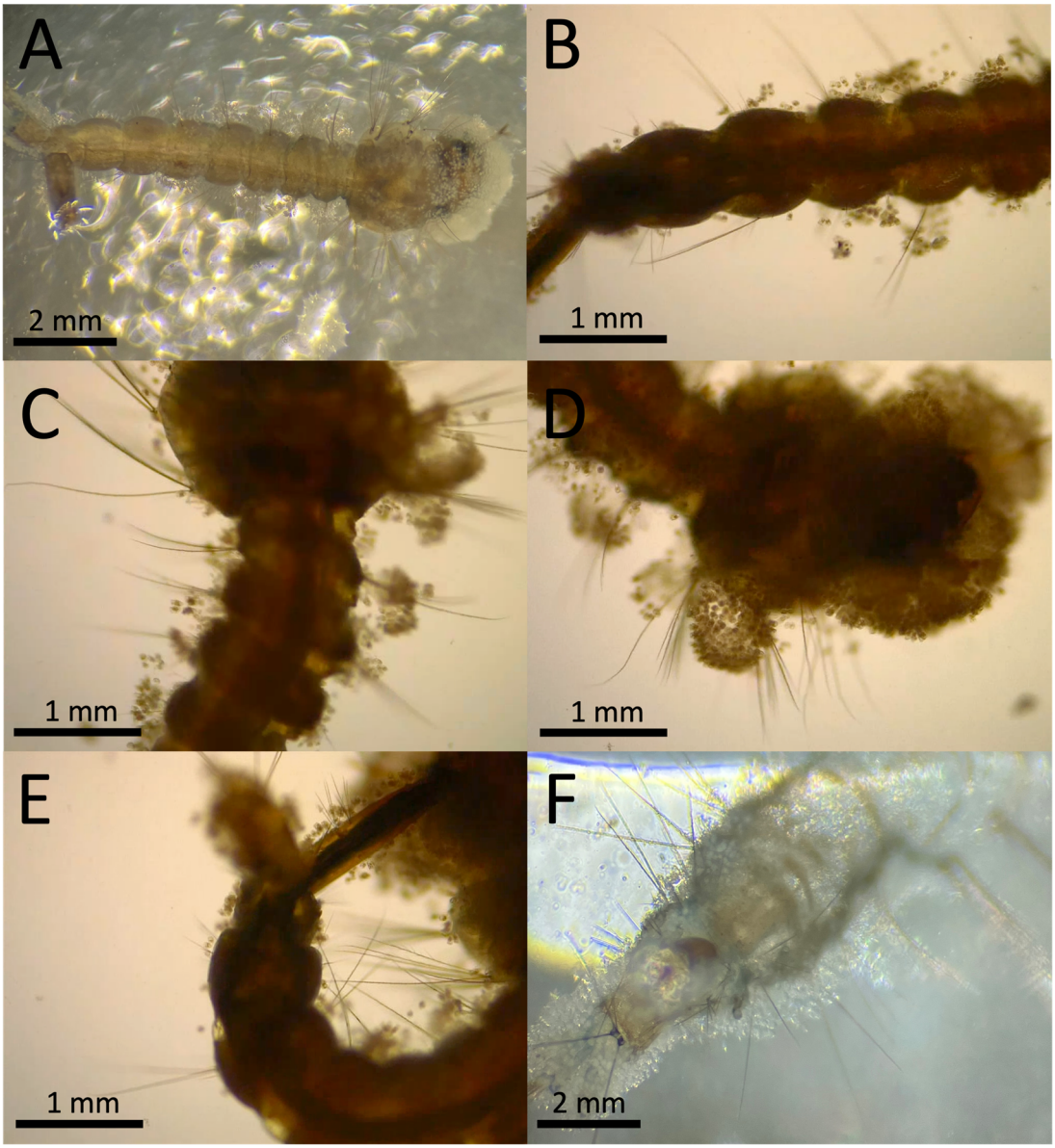

Figure 2. Representative images (A-E) of heavily infected *Culex quinquefasciatus* larva. (F) Heavy infection on empty larval exuvia..

 doi:10.20944/preprints202402.1594.v1

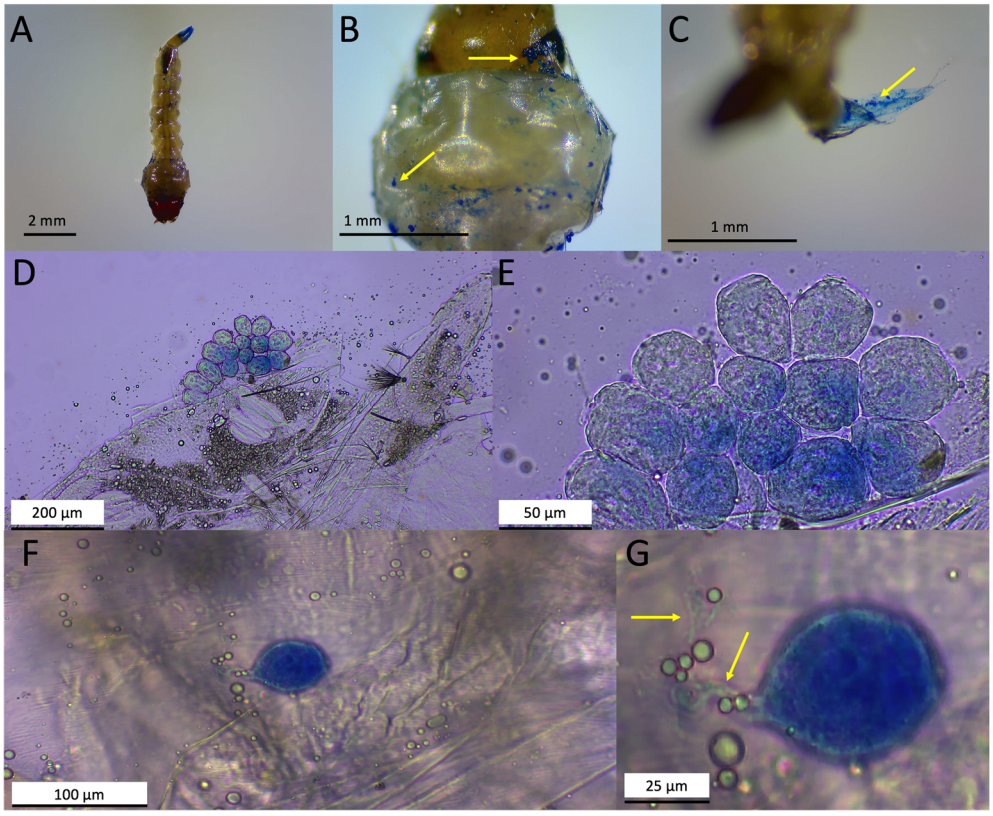

Figure 3. Representative images of infected mosquito larvae stained with lactophenol cotton blue dye and imaged using a dissecting microscope **(A-C)** and a compound microscope **(D-G)**. **(A)** Whole stained mosquito larva showing clusters of blue infection structures (potentially encysted zoospores) along the body. **(B)** Higher magnification image of infection structures (arrows) clustered around the head of the larva. **(C)** Higher magnification of infection structures (arrows) clustered around the siphon of the larva. **(D)** Mosquito larvae were crushed onto a microscope slide and examined at 100X oil immersion using a compound microscope. Encysted zoospores are evident in a cluster along the body of the larva. **(E)** Higher magnification image of encysted zoospores showing gross morphology. **(F)** Single isolated zoospore cyst. **(G)** Infection and attachment structures evident on isolated cyst (arrows).

 doi:10.20944/preprints202402.1594.v1

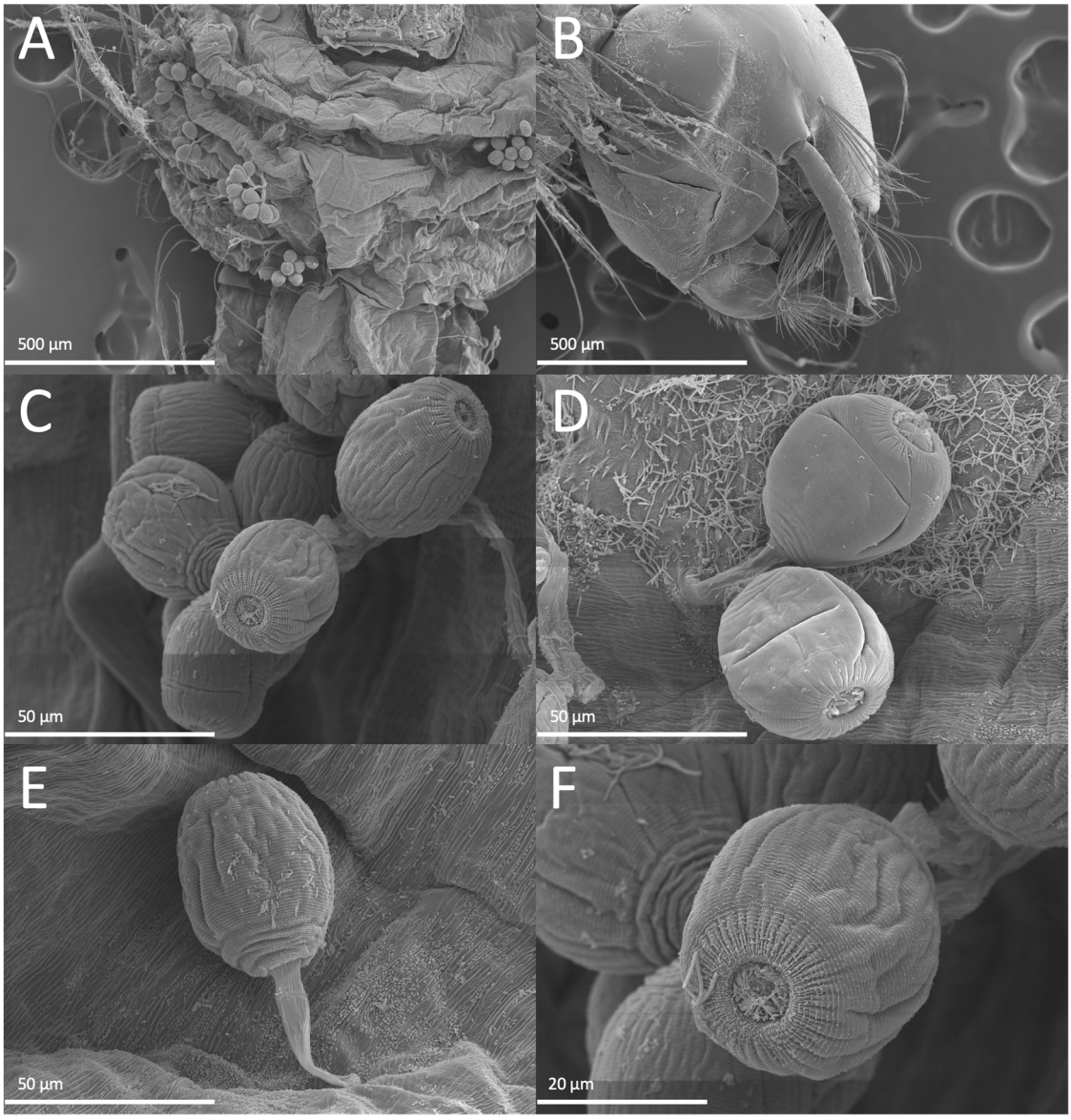

Figure 4. Representative images of scanning electron microscopy (SEM) analyses of infected mosquito larvae. **(A)** Encysted zoospores clustered along the underside of the mosquito larva head. **(B)** Microbial attachment and infection structures along the head. **(C)** Cluster of encysted zoospores appearing slightly oblong with shriveled lines along their sides and a distinct pore-like structure opposite to the attached end. **(D)** Two zoospore cysts attached (attachment structure visible) to the surface of the larva. **(E)** Profile of single zoospore, showing the attachment/infection structure and side morphology of the cyst. **(F)** Single zoospore cyst from a top view showing the pore-like structure at the top of the cyst.

Samples II & III: collected 11/15/2022 (Nursery Ln & Park Ln). Three infected mosquito larvae were chosen at random for isolation of the infectious agent by hyphal tipping as described above. Isolates were then purified via hyphal tipping and successive passage (3 times) of single colonies on PDA amended with streptomycin and ampicillin, resulting in isolates LCMP-T1, LCMP-T2, and LCMP-T3.

Phenotypic and molecular characterization of LCMP-P1- Pythium thermoculicivorax

LCMP-P1 showed robust vegetative growth on a variety of media including PDA (Fig. 5A), SDA, and CZA at 24°C. On PDA, colonies appeared white to off-white, flattened, with a wet appearance and crenelated edges (Fig. 5A). This isolate was observed to grow at an average rate of 18.93 mm/day

 doi:10.20944/preprints202402.1594.v1

on PDA. Examination of hyphal growth after lactophenol cotton blue staining showed sporangia forming on branched structures and mature sporangia within and developing at the ends of growing hyphae (Fig. 5B & C). Growing filamentous hyphal structures showed high levels of internal vesicles, typical of many *Pythium* species, as well as sporangial structures that were globose with plurotic oospores (Fig. 5D & E). Thermal tolerance experiments in which PDA plates were incubated at different temperatures revealed that the isolate was temperature resistant showing robust vegetative growth at 30°C and 37°C, similar to that seen at 25°C, although it was noted that the distinct crenelations seen at 24°C appeared to be increasingly smoothened at the higher temperatures (Fig. 6).

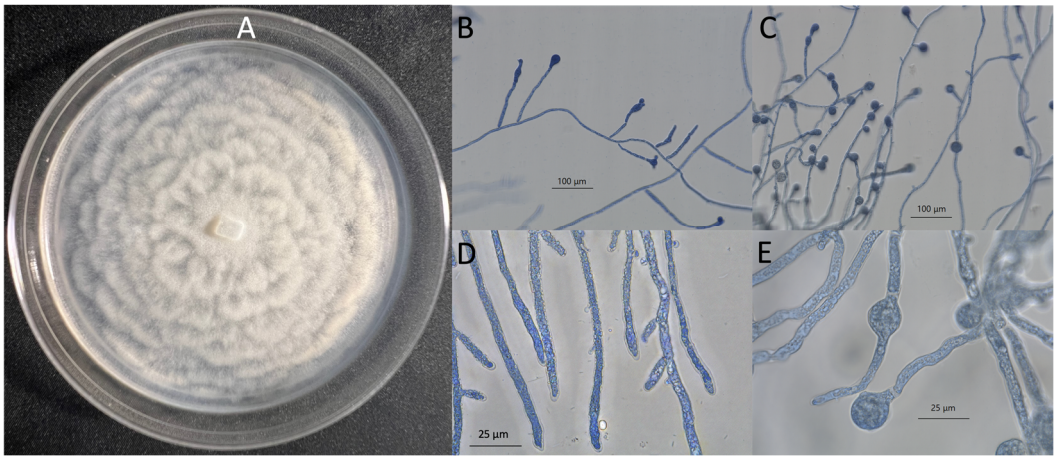

Figure 5. Isolate LCMP-P1 (*Pythium*) plate and hyphal morphology. **(A)** Plate morphology of the *Pythium* isolate grown on PDA at 24°C for 7 days. **(B)** *Pythium* hyphae stained by lactophenol cotton blue showing sporangia forming on branched structures. **(C)** Mature sporangia forming from hyphae. **(D)** Close-up of hyphae showing gross morphology. **(E)** Close-up of sporangial structures.

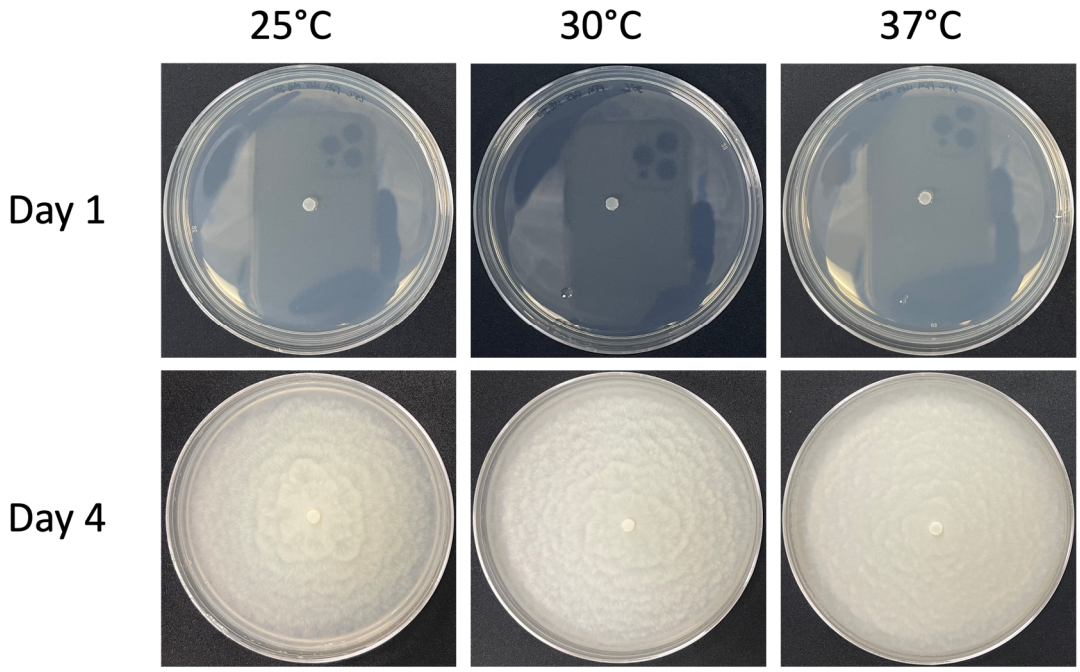

Figure 6. Temperature profile of Isolate LCMP-P1 (*Pythium*) growth on PDA plates. Isolate LCMP-P1 was inoculated into the center of PDA plates in triplicate and grown at 3 different temperatures (25°C, 30°C, and 37°C) and allowed to grow for 4 days, with plates photographed at 1 d and 4 d post-inoculation.

 doi:10.20944/preprints202402.1594.v1

Characteristics: Sporangia globosa and subglobosa, intercalaria, terminalia, 15-25 µm diameter, zoospores not observed. Oogonia globosa, intercalaria, terminalia, 16-20 µm diameter. Mycelium hyaline, moderately branched, 4-7 µm wide. Antheridia were sparsely noted in association with oogonia and took the form of short sections of hyphae which branched from the main hyphal strand just before an oogonium and then fused with oogonia, sometimes with a swollen end at the attachment site.

To establish the identity of this isolate genomic DNA was extracted from growing mycelia and the ITS and mitochondrial *COX1* loci were amplified and sequenced as detailed in the Methods section. A combined maximum likelihood phylogenetic tree of 653 bp of the combined ITS and LSU (accession # PP262616) regions and 672 bp of the *COX1* (accession #PP107950) loci with sequences from related species confirmed placement of the isolate within the *Pythium* genus, with *P. inflatum* CBS16868 being the closest neighbor in the tree and showing the highest sequence similarity in a BLAST search (95.17%), although the isolate was distinct from the latter (Fig. 7).

Etymology: Due to its mosquito larval pathogen and thermal tolerance phenotypes, the isolate is being named *P. thermoculicovorax*.

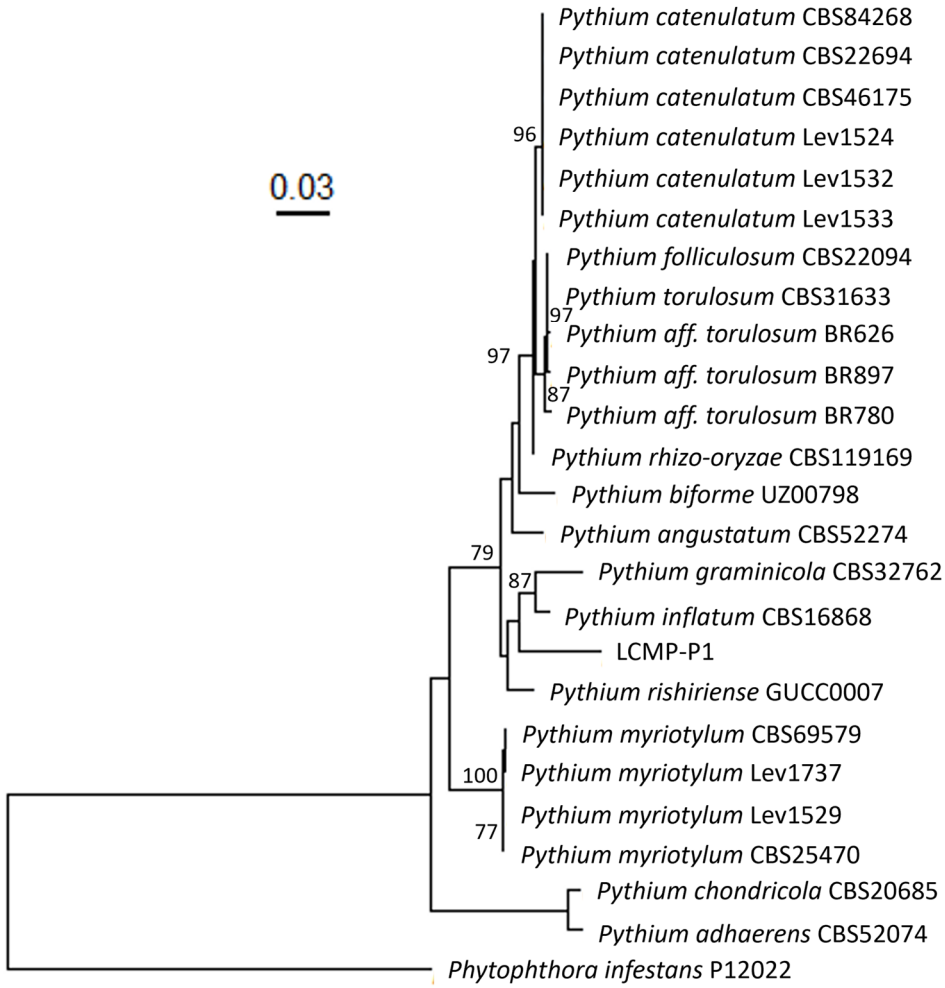

Figure 7. Maximum likelihood phylogenetic tree of combined ITS and COX1 loci of the *Pythium* isolate LCMP-P1 collected in this study and closely related *Pythium* species. BLAST searches of this isolate showed sequence similarity to Clade B *Pythium* species. Sequences of closely related *Pythium* species within this clade, and several from different clades (*Pythium chondricola* CBS20685 and *Pythium adhaerens* CBS52074) were obtained from Genbank for both loci and used to generate phylogenetic trees. Phylogenies were generated using RAxML with 2000 bootstrap replicates. The *Pythium* isolate collected in this study appears to cluster most closely with *Pythium inflatum* CBS16868, but forms a

 doi:10.20944/preprints202402.1594.v1

distinct branch, suggesting high levels of sequence divergence between these two strains. *Phytophthora infestans* P12022 was used as an outgroup. Bootstrap support values >70 are displayed on the tree. Tip labels display species name and strain.

Characterization of isolates LCMP-T1, LCMP-T2, and LCMP-T3- Trichoderma sp.

Isolates LCMP-T1, LCMP-T2, and LCMP-T3 all grew robustly on PDA, with the colonies of LCMP-T2 and LCMP-T3 turning green after 6-7 d of growth at 24°C (Fig. 8A-J), becoming progressively darker green after 7 d of growth. These isolates grew at average rates of 24.04 and 26.7 mm/day on PDA, respectively. Isolate LCMP-T1 was slower growing and the colony color was white after 7 d of growth (Fig. 8K-O) and remained white to very pale green at 14 d. This isolate grew at an average rate of 23.46 mm/day on PDA. Lactophenol blue staining of growing vegetative cells of LCMP-T2 showed extensive branched hyphae and mycelia, with green conidial spores apparent (Fig. 8B-E). Similarly, green conidial spores were apparent for LCMP-T3 (Fig. 8G-J). LCMP-T1 hyphae were hyaline and showed obvious septa and swollen terminal structures, with fewer spores that remained colorless (unless stained by the lactophenol blue) (Fig. 8L-O).

 doi:10.20944/preprints202402.1594.v1

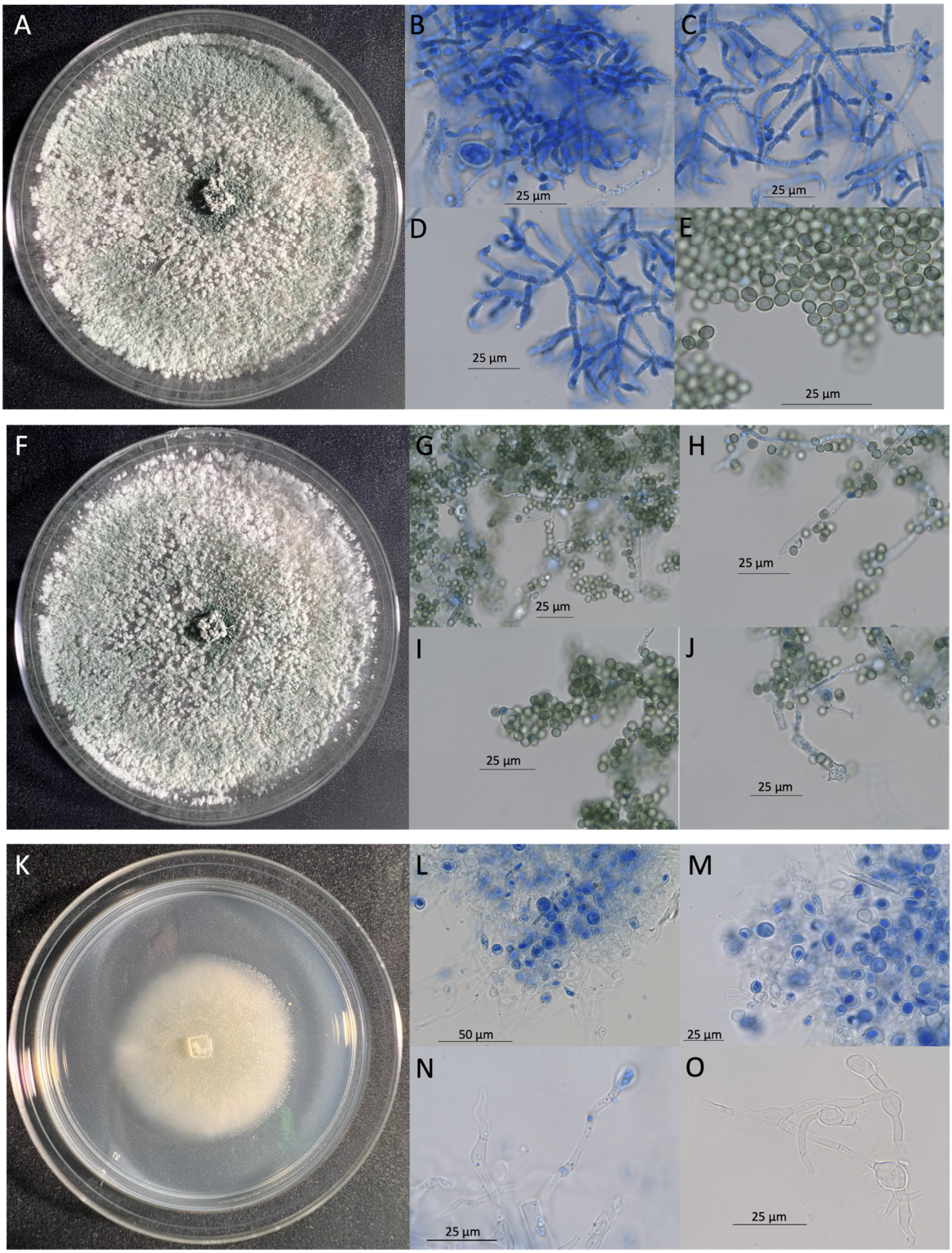

Figure 8. Plate and hyphal and conidial morphologies of Isolates LCMP-T2 **(A-E)**, LCMP-T3 **(F-J)**, and LCMP-T1 **(K-O)**. **(A, F, K)** Plate morphologies on PDA at 24°C 7 d. **(B, C, D)** Hyphae stained with lactophenol cotton blue, **(E)** green pigmented conidial spores, **(G)** lactophenol blue-stained hyphae and spores. **(H)** terminal hyphae showing septa and spores showing green pigmentation, **(I)** spores and potential conidiophore, **(J)** hyphae showing vesicles, potential conidiophore, and spores, **(L)** lactophenol blue stained hyphae, **(M)** clumps of stained hyphae showing swollen terminal structures, **(N)** isolated hyphae showing septa and swollen terminal structures, **(O)** hyphae showing swollen interior and terminal structures.

 doi:10.20944/preprints202402.1594.v1

To establish the identities of these isolates, genomic DNA was extracted from growing vegetative cells, and the ITS (LCMP-T1 accession #PP125838, LCMP-T2 accession #PP125839, LCMP-T3 accession #PP125840), *TEF1a (*LCMP-T1 accession #PP178665, LCMP-T2 accession #PP178663, LCMP-T3 accession #PP178664), and *RBP2 (*LCMP-T1 accession #PP178660, LCMP-T2 accession #PP178661, LCMP-T3 accession #PP178662) loci amplified and sequenced as detailed in the Methods section. Sequences were concatenated and used for construction of a phylogenetic tree with closely related sequences as determined by BLAST searches of the NCBI database (Fig. 9). These data showed that all three isolates clustered within *Trichoderma* sp., with isolates LCMP T2 and LCMP-T3 appearing closely related to each other and clustering with *T. asperellum* (99.84% identity) and Isolate LCMP-T1 clustering most closely with *T. strigosum* (98.19% identity).

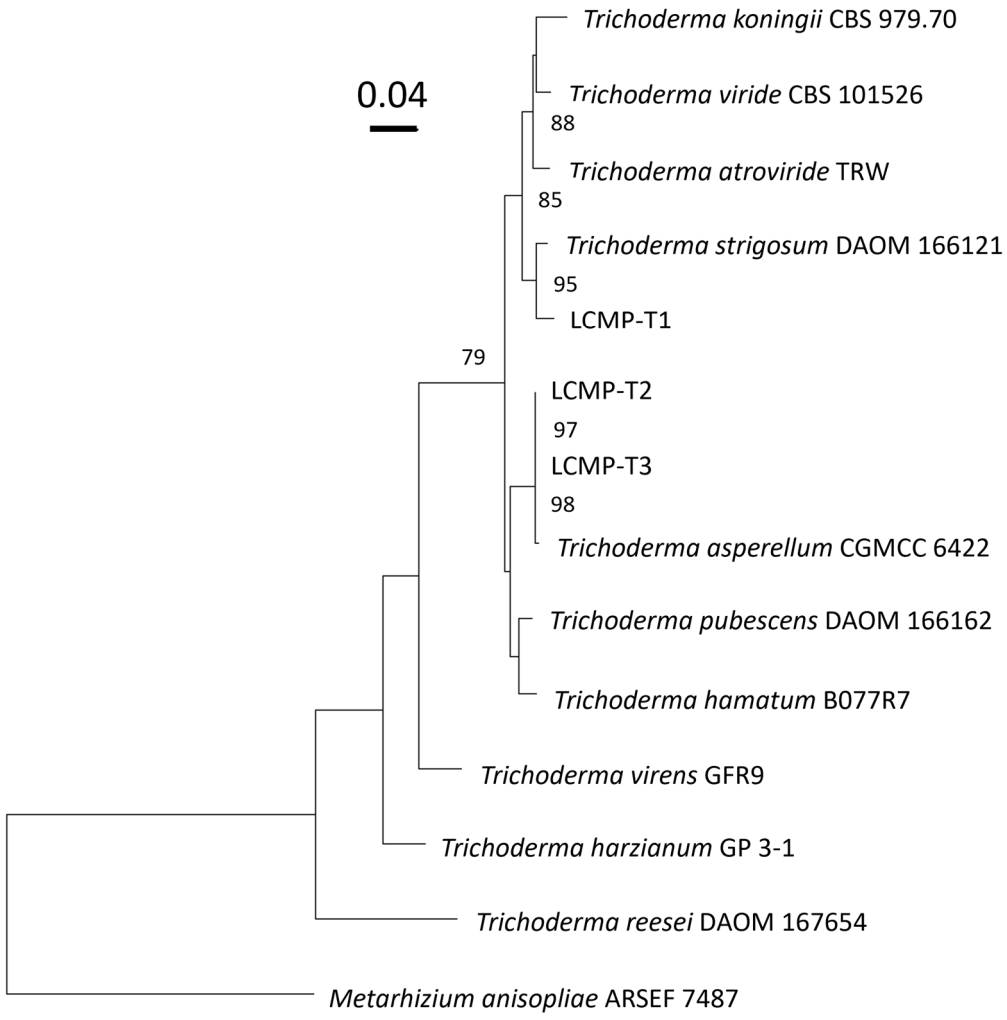

Figure 9. Maximum likelihood phylogenetic tree of ITS, TEF1a, and RPB2 sequences of Isolates LCMP-T1, LCMP-T2, and LCMP-T3 with closely related *Trichoderma* species. Sequences for closely related species at each of the three loci were obtained from Genbank. The phylogenetic tree was generated using RAxML with 2000 boostrap relicates. In this tree, LCMP-T1 is seen to cluster most closely with *Trichoderma strigosum* while isolates LCMP-T2 and LCMP-T3 formed a cluster closely with *Trichoderma asperellum*. *Metarhizium anisopliae* ARSEF 7487 was used as an outgroup in the generation of this tree. Bootstrap support values >70 are displayed on the tree. Tip labels display species name and strain.

P. thermoculcivorax zoospores

 doi:10.20944/preprints202402.1594.v1

Zoospores were not observed from standard culture media, however, after growth on V8 agar medium for 5-7 days, followed by excision of a block of actively growing hyphae from the edge of a colony and immersion in sterilized tap water for 3 hours to 3 days, a small number of zoospores were apparent (Supplemental Fig. S1). These zoospores appeared oblong, with one end tapering slightly while the other end remained rounded and with two central organellar structures consistently noted in the center of the cells, with biflagellate structures visible and the cells were motile (Supplemental Videos S1-S3).

4. Discussion

Chemical pesticides continue to be the most widely used method for mosquito control, although alternatives, including natural products, gene targeting, sterile insect technique and biological agents such as mosquito pathogenic viruses, bacteria, and fungi are actively being examined and some even commercialized for mosquito control [15,44–49]. Methods for facile isolation of microbial mosquito larval pathogens ranging from fungi to oomycetes have led to identification of several new species [50–52]. Of note, use of many of these biological agents is both compatible with (though not necessarily needed) and capable of targeting insecticide resistant insect populations, with little to no evidence of the emergence of resistance to the (fungal) agent [17,18,20,53–56].

The temperate and subtropical climate zones, coupled to high humidity and presence of significant bodies of relatively static fresh water (swamps) in Florida (USA) has long been recognized as an ideal breeding ground for mosquitoes and the (human and animal) disease-causing agents they carry. Despite the abundance of mosquitoes found, studies examining mosquito enzootic infections in Florida have been few. Here, we observed a series of natural enzootic outbreaks in several mosquito populations in Southwest Florida from 2021-2023. Mosquito larvae sampled from these sites had a large amount of microbial growth that could be readily seen by eye and confirmed via microscopy. Three sites containing infected *Ps. columbiae* larvae were used for isolation of the infectious microbe via hyphal tipping on PDA plates, resulting in four strains designated as Isolates LCMP-P1, LCMP-T1, LCMP-T2, and LCMP-T3. Initial imaging of mosquitoes infected by Isolate LCMP-P1 was consistent with an oomycete as the infectious agent due to the observance of cells consistent with zoospore cysts. This was further confirmed via SEM high resolution morphological characterization of LCMP-P1 that showed clusters of encysted zoospores throughout the infected mosquito larvae, although concentrated at the head and siphon regions. The encysted zoospores displayed a unique morphology, with radial striations and a pore distal to the attachment tube. To the best of our knowledge these are the first images of this sort of oomycete infection of mosquito larvae. LCMP-P1 grew rapidly in culture and formed characteristic hyphae and sporangia consistent with those seen for many *Pythium* species. The nucleotide sequences of the nuclear ITS and mitochondrial COX1 loci were determined and used to construct a concatenated phylogenetic tree, establishing the identity of the isolate within the *Pythium* genus. This isolate grouped most closely to *P. inflatum*, however, it formed a distinct branch from this taxon. *P. inflatum* has been implicated as a pathogen of a number of crop plants including strawberry, corn, and soybean, and has been isolated from soil and water samples in Africa and Korea [57–60], however, its description as an invertebrate or mosquito larval pathogen has not been reported.

Although mainly characterized as plant pathogens [61–63], various oomycete (in classic literature referred to as water molds) strains are also known for their human/mammalian pathogenicity (e.g., *P. insidiosum*) [64–66], and, within this context, several oomycete mosquito (facultative) pathogens have also been described. *Lagenidium giganteum* was briefly registered by the US Environmental Protection Agency for mosquito larval control, however, reports of potential life-threatening cases in dogs derailed its use [28,67,68]. *Leptolegnia chapmanii* has been shown to be pathogenic to various mosquito larvae with methods for their detection in infected *Aedes aegypti* (L., 1762) larvae reported [30,51]. Various *Pythium* species as well as one *Saprolegnia* sp. have been characterized as mosquito larval pathogens from soil samples [69], and an earlier report of a *Pythium* isolate causing high mortality in field-collected larvae of *Aedes sierrensis* (Lynch-Arribalzaga, 1891), reported motile zoospores as the infective stage that were strongly chemotactic to mosquito larvae

 doi:10.20944/preprints202402.1594.v1

wounds [22]. Comparative genomic and transcriptomic analyses of the mosquito larval oomycete pathogen, *P. guiyangense*, has yielded insights into infection mechanisms and its putative virulence and effector repertoire, the putative roles of chitinases and tyrosine kinases [36,70]. In addition, preliminary molecular studies identified a ser/thr-protein (AGC-) kinase family member, that includes the PKA cAMP-dependent protein kinases, in vegetative growth, stress response, and virulence [71].

As mentioned, the mammalian pathogen, *P. insidiosum*, has also been isolated from infected mosquito larvae, with the investigated isolate capable of growing at 37°C [35]. Intriguingly, the *Pythium* isolate described herein was also thermotolerant, capable of almost equivalent growth at 25°C, 30°C, and 37°C. Because of this property and due to its (ITS and COXI sequence) divergence from its nearest characterized relative, *P. inflatum*, originally isolated from vegetative debris [72] and considered a plant (corn, strawberry, soybean) pathogen [73], we have designated our isolate as *P. thermoculicivorax*. Subsequent sampling at two different sites of infected *Ps. columbiae* larvae resulted in the identification of three *Trichoderma* isolates (Isolates LCMP-T1-3). Phylogenetic analyses using three loci, namely, ITS, *TEF1a*, and *RBP2* sequences grouped Isolate LCMP-T1 as closely related to *T. strigosum*. Isolates LCMP-T2 and 3, were found to be closely related to their closest phylogenetic neighbor, *T. asperellum*. A number of *Trichoderma* species have been identified as insect pathogens [74], although thus far not *T. strigosum*, which has apparently been mainly isolated from soil as a potential plant protective species [75–77]. Isolates of *T. asperellum* appear to be more diverse in their biology, with several characterized as displaying plant protective qualities capable of offering protection against plant pathogenic fungi including *Fusarium*, *Botrytis*, and *Phellinus* sp., that cause various rot, wilt, and mildew diseases in agricultural crops and trees [78–82]. *Trichoderma asperellum* has been applied in conjunction with the insect pathogenic fungus, *Beauveria bassiana* (Bals.-Criv, 1835), in attempts to protect maize from the Asian corn borer (*Ostrinia furnacalis* (Guenee, 1854)) [83], and its nematocidal potential has also been reported [84]. *Trichoderma asperellum* has also been implicated as an anopheline larvicide [85], and cell wall degrading extracts from the fungus have shown larvicidal activity against *Ae. aegypti* [86]. Our data highlight the potential diversity and importance of examining enzootic infections in target insect species that can lead to novel pathogen discovery that may have important impacts in natural insect populations as well as a resource or reservoir for isolation of potential (mosquito) biological control agents.

Supplementary Materials: The following supporting information can be downloaded at the website of this paper posted on Preprints.org, Figure S1: Zoospores imaged in culture; Table S1: Locations where infected larvae were noted. Table S2: Primers used to amplify loci from *Pythium* and *Trichoderma* isolates; Table S3 and S4: Genbank IDs of species and loci used for generating phylogenic trees; Video S1: Motile zoospores; Video S2: Zoospore with flagella visible; Video S3: Zoospore with flagella visible.

Author Contributions: Conceptualization, RJ, CD, DH, and NOK; methodology, RJ and CD; validation and analysis, RJ, CD AL, DH, and NOK.; investigation, RJ and CD; resources, AL, DG, and NOK; writing—RJ, CD, and NOK.; writing, review and editing—AL and DH; visualization, RJ, CD, and NOK; supervision, AL, DH, and NOK; project administration, AL, DH, and NOK; funding acquisition, AL, DH, and NOK. All authors have read and agreed to the published version of the manuscript.

Funding: This research was funded in part by USDA-NIFA, grant award number 2020-67013-31268 to NOK and NSF-IOS, grant number 2418026 to NOK.

Data Availability Statement: All data are available publicly and/or are included in the manuscript and Supporting data sections.

Conflicts of Interest: The authors declare no conflicts of interest. The funders had no role in the design of the study; in the collection, analyses, or interpretation of data; in the writing of the manuscript; or in the decision to publish the results.

References

1. Glare, T.; Caradus, J.; Gelernter, W.; Jackson, T.; Keyhani, N.; Kohl, J.; Marrone, P.; Morin, L.; Stewart, A. Have biopesticides come of age? *Trends Biotechnol.* **2012**, *30*, 250-258, doi:10.1016/j.tibtech.2012.01.003.

2. Marrone, P.G. Status of the biopesticide market and prospects for new bioherbicides. *Pest Manag Sci* **2023**, doi:10.1002/ps.7403.
3. Koller, J.; Sutter, L.; Gonthier, J.; Collatz, J.; Norgrove, L. Entomopathogens and Parasitoids Allied in Biocontrol: A Systematic Review. *Pathogens* **2023**, *12*, doi:10.3390/pathogens12070957.
4. Elya, C.; De Fine Licht, H.H. The genus Entomophthora: bringing the insect destroyers into the twenty-first century. *Ima Fungus* **2021**, *12*, 34, doi:10.1186/s43008-021-00084-w.
5. Kyle, C.H.; Liu, J.; Gallagher, M.E.; Dukic, V.; Dwyer, G. Stochasticity and Infectious Disease Dynamics: Density and Weather Effects on a Fungal Insect Pathogen. *Am. Nat.* **2020**, *195*, 504-523, doi:10.1086/707138.
6. Lacey, L.A.; Grzywacz, D.; Shapiro-Ilan, D.I.; Frutos, R.; Brownbridge, M.; Goettel, M.S. Insect pathogens as biological control agents: Back to the future. *J. Invertebr. Pathol.* **2015**, *132*, 1-41, doi:10.1016/j.jip.2015.07.009.
7. Touray, M.; Bakirci, S.; Ulug, D.; Gulsen, S.H.; Cimen, H.; Yavasoglu, S.I.; Simsek, F.M.; Ertabaklar, H.; Ozbel, Y.; Hazir, S. Arthropod vectors of disease agents: Their role in public and veterinary health in Turkiye and their control measures. *Acta Trop.* **2023**, *243*, 106893, doi:10.1016/j.actatropica.2023.106893.
8. Onen, H.; Luzala, M.M.; Kigozi, S.; Sikumbili, R.M.; Muanga, C.K.; Zola, E.N.; Wendji, S.N.; Buya, A.B.; Balciunaitiene, A.; Viskelis, J.; et al. Mosquito-Borne Diseases and Their Control Strategies: An Overview Focused on Green Synthesized Plant-Based Metallic Nanoparticles. *Insects* **2023**, *14*, doi:10.3390/insects14030221.
9. Giunti, G.; Becker, N.; Benelli, G. Invasive mosquito vectors in Europe: From bioecology to surveillance and management. *Acta Trop.* **2023**, *239*, 106832, doi:10.1016/j.actatropica.2023.106832.
10. Duval, P.; Antonelli, P.; Aschan-Leygonie, C.; Valiente Moro, C. Impact of Human Activities on Disease-Spreading Mosquitoes in Urban Areas. *J. Urban Health* **2023**, *100*, 591-611, doi:10.1007/s11524-023-00732-z.
11. Arnal, A.; Roche, B.; Gouagna, L.C.; Dujon, A.; Ujvari, B.; Corbel, V.; Remoue, F.; Poinsignon, A.; Pompon, J.; Giraudeau, M.; et al. Cancer and mosquitoes - An unsuspected close connection. *Sci. Total Environ.* **2020**, *743*, 140631, doi:10.1016/j.scitotenv.2020.140631.
12. Vatandoost, H.; Hanafi-Bojd, A.A.; Nikpoor, F.; Raeisi, A.; Abai, M.R.; Zaim, M. Situation of insecticide resistance in malaria vectors in the World Health Organization of Eastern Mediterranean region 1990-2020. *Toxicol Res (Camb)* **2022**, *11*, 1-21, doi:10.1093/toxres/tfab126.
13. Tepa, A.; Kengne-Ouafo, J.A.; Djova, V.S.; Tchouakui, M.; Mugenzi, L.M.J.; Djouaka, R.; Pieme, C.A.; Wondji, C.S. Molecular Drivers of Multiple and Elevated Resistance to Insecticides in a Population of the Malaria Vector Anopheles gambiae in Agriculture Hotspot of West Cameroon. *Genes (Basel)* **2022**, *13*, doi:10.3390/genes13071206.
14. Sonhafouo-Chiana, N.; Nkahe, L.D.; Kopya, E.; Awono-Ambene, P.H.; Wanji, S.; Wondji, C.S.; Antonio-Nkondjio, C. Rapid evolution of insecticide resistance and patterns of pesticides usage in agriculture in the city of Yaounde, Cameroon. *Parasit Vectors* **2022**, *15*, 186, doi:10.1186/s13071-022-05321-8.
15. Meier, C.J.; Rouhier, M.F.; Hillyer, J.F. Chemical Control of Mosquitoes and the Pesticide Treadmill: A Case for Photosensitive Insecticides as Larvicides. *Insects* **2022**, *13*, doi:10.3390/insects13121093.
16. Katak, R.M.; Cintra, A.M.; Burini, B.C.; Marinotti, O.; Souza-Neto, J.A.; Rocha, E.M. Biotechnological Potential of Microorganisms for Mosquito Population Control and Reduction in Vector Competence. *Insects* **2023**, *14*, doi:10.3390/insects14090718.
17. Howard, A.F.V.; N'Guessan, R.; Koenraadt, C.J.M.; Asidi, A.; Farenhorst, M.; Akogbeto, M.; Thomas, M.B.; Knols, B.G.J.; Takken, W. The entomopathogenic fungus *Beauveria bassiana* reduces instantaneous blood feeding in wild multi-insecticide-resistant *Culex quinquefasciatus* mosquitoes in Benin, West Africa. *Parasite Vector* **2010**, *3*, -.
18. Howard, A.F.V.; Koenraadt, C.J.M.; Farenhorst, M.; Knols, B.G.J.; Takken, W. Pyrethroid resistance in *Anopheles gambiae* leads to increased susceptibility to the entomopathogenic fungi *Metarhizium anisopliae* and *Beauveria bassiana*. *Malaria Journal* **2010**, *9*, -.
19. Scholte, E.J.; Knols, B.G.; Samson, R.A.; Takken, W. Entomopathogenic fungi for mosquito control: a review. *J. Insect Sci.* **2004**, *4*, 19, doi:10.1093/jis/4.1.19.
20. Bilgo, E.; Lovett, B.; Bayili, K.; Millogo, A.S.; Sare, I.; Dabire, R.K.; Sanon, A.; St Leger, R.J.; Diabate, A. Transgenic Metarhizium pingshaense synergistically ameliorates pyrethroid-resistance in wild-caught, malaria-vector mosquitoes. *Plos One* **2018**, *13*, doi:ARTN e0203529 10.1371/journal.pone.0203529.
21. Fang, W.G.; Vega-Rodriguez, J.; Ghosh, A.K.; Jacobs-Lorena, M.; Kang, A.; St Leger, R.J. Development of transgenic fungi that kill human malaria parasites in mosquitoes. *Science* **2011**, *331*, 1074-1077.
22. Clark, T.B.; Kellen, W.R.; Lindegren, J.E.; Sanders, R.D. *Pythium* sp. (Phycomycetes:Pythiales) pathogenic to mosquito larvae. *J. Invertebr. Pathol.* **1966**, *8*, 351-354.
23. Seymour, R.L. *Leptolegnia Chapmanii*, an oomycete pathogen of mosquito larvae. *Mycologia* **1984**, *76*, 670-674.
24. Vilela, R.; Humber, R.A.; Taylor, J.W.; Mendoza, L. Phylogenetic and physiological traits of oomycetes originally identified as Lagenidium giganteum from fly and mosquito larvae. *Mycologia* **2019**, *111*, 408-422, doi:10.1080/00275514.2019.1589316.

25. Lord, J.C.; Roberts, D.W. Effects of salinity, pH, organic solutes, anaerobic conditions, and the presence of other microbes on production and survival of Lagenidium giganteum (Oomycetes: Lagenidiales) zoospores. *J. Invertebr. Pathol.* **1985**, *45*, 331-338, doi:10.1016/0022-2011(85)90111-9.
26. Kerwin, J.L.; Washino, R.K. Field evaluation of Lagenidium giganteum (Oomycetes: Lagenidiales) and description of a natural epizootic involving a new isolate of the fungus. *J. Med. Entomol.* **1988**, *25*, 452-460, doi:10.1093/jmedent/25.6.452.
27. Kerwin, J.L. Oomycetes: Lagenidium giganteum. *J. Am. Mosq. Control Assoc.* **2007**, *23*, 50-57, doi:10.2987/8756-971X(2007)23[50:OLG]2.0.CO;2.
28. Vilela, R.; Taylor, J.W.; Walker, E.D.; Mendoza, L. Lagenidium giganteum pathogenicity in mammals. *Emerg Infect Dis* **2015**, *21*, 290-297, doi:10.3201/eid2102.141091.
29. Spies, C.F.J.; Grooters, A.M.; Levesque, C.A.; Rintoul, T.L.; Redhead, S.A.; Glockling, S.L.; Chen, C.Y.; de Cock, A. Molecular phylogeny and taxonomy of Lagenidium-like oomycetes pathogenic to mammals. *Fungal Biol* **2016**, *120*, 931-947, doi:10.1016/j.funbio.2016.05.005.
30. Lord, J.C.; Fukuda, T. An ultrastructural study of the invasion of Culex quinquefasciatus larvae by Leptolegnia chapmanii (Oomycetes: Saprolegniales). *Mycopathologia* **1988**, *104*, 67-73, doi:10.1007/BF00436929.
31. Pelizza, S.A.; Scorsetti, A.C.; Lastra, C.C.; Garcia, J.J. Production of oogonia and oospores of Leptolegnia chapmanii Seymour (Straminipila: Peronosporomycetes) in Aedes aegypti (L.) larvae at different temperatures. *Mycopathologia* **2010**, *169*, 71-74, doi:10.1007/s11046-009-9224-6.
32. Paramo, M.E.R.; Falvo, M.; Garcia, J.; Lastra, C.C.L. Compatibility between Leptolegnia chapmanii and diflubenzuron and neem oil for the control of Aedes aegypti. *Rev Argent Microbiol* **2020**, *52*, 240-244, doi:10.1016/j.ram.2019.10.001.
33. Su, X.; Zou, F.; Guo, Q.; Huang, J.; Chen, T. A report on a mosquito-killing fungus, Pythium carolinianum. *Fungal Diversity* **2001**, *7*, 129-133.
34. Huang, S.-W.; Su, X.-Q. Biological Studies on Pythium guiyangense, a fungal pathogen of mosquito larvae. *Mycosystema* **2007**, *23*, 380-388.
35. Vilela, R.; Montalva, C.; Luz, C.; Humber, R.A.; Mendoza, L. Pythium insidiosum isolated from infected mosquito larvae in central Brazil. *Acta Trop.* **2018**, *185*, 344-348, doi:10.1016/j.actatropica.2018.06.014.
36. Shen, D.; Dong, Y.; Wei, Y.; Zhang, M.; Wang, J.; Tang, Z.; Xia, Q.; Nyawira, K.T.; Jing, M.; Dou, D.; et al. Genome-wide and functional analyses of tyrosine kinase-like family genes reveal potential roles in development and virulence in mosquito pathogen Pythium guiyangense. *Fungal Genet. Biol.* **2019**, *130*, 11-18, doi:10.1016/j.fgb.2019.04.009.
37. Shen, D.; Tang, Z.; Wang, C.; Wang, J.; Dong, Y.; Chen, Y.; Wei, Y.; Cheng, B.; Zhang, M.; Grenville-Briggs, L.J.; et al. Infection mechanisms and putative effector repertoire of the mosquito pathogenic oomycete Pythium guiyangense uncovered by genomic analysis. *PLoS Genet.* **2019**, *15*, e1008116, doi:10.1371/journal.pgen.1008116.
38. Darsie Jr, R.F.; Ward, R.A. *Identification and geographic distribution of the mosquitoes of North America, north of Mexico*; University of Florida Press: Gainesville, FL, 2005.
39. Dou, K.; Lu, Z.; Wu, Q.; Ni, M.; Yu, C.; Wang, M.; Li, Y.; Wang, X.; Xie, H.; Chen, J.; et al. MIST: a Multilocus Identification System for Trichoderma. *Appl. Environ. Microbiol.* **2020**, *86*, doi:10.1128/AEM.01532-20.
40. Robideau, G.P.; De Cock, A.W.; Coffey, M.D.; Voglmayr, H.; Brouwer, H.; Bala, K.; Chitty, D.W.; Desaulniers, N.; Eggertson, Q.A.; Gachon, C.M.; et al. DNA barcoding of oomycetes with cytochrome c oxidase subunit I and internal transcribed spacer. *Mol Ecol Resour* **2011**, *11*, 1002-1011, doi:10.1111/j.1755-0998.2011.03041.x.
41. Castresana, J. Selection of conserved blocks from multiple alignments for their use in phylogenetic analysis. *Mol. Biol. Evol.* **2000**, *17*, 540-552, doi:10.1093/oxfordjournals.molbev.a026334.
42. Stamatakis, A. RAxML version 8: a tool for phylogenetic analysis and post-analysis of large phylogenies. *Bioinformatics* **2014**, *30*, 1312-1313, doi:10.1093/bioinformatics/btu033.
43. Yu, G.; Smith, D.; Zhu, H.; Guan, Y.; Lam, T.T.Y. ggtree: an R package for visualization and annotation of phylogenetic trees with different types of meta-data. *Methods in Ecology and Evolution* **2024**.
44. Yadav, M.; Dahiya, N.; Sehrawat, N. Mosquito gene targeted RNAi studies for vector control. *Funct Integr Genomics* **2023**, *23*, 180, doi:10.1007/s10142-023-01072-6.
45. Rodrigues Dos Santos, D.; Lopes Chaves, L.; Couto Pires, V.; Soares Rodrigues, J.; Alves Siqueira de Assuncao, M.; Bezerra Faierstein, G.; Gomes Barbosa Neto, A.; de Souza Reboucas, J.; Christine de Magalhaes Cabral Albuquerque, E.; Alexandre Beisl Vieira de Melo, S.; et al. New weapons against the disease vector Aedes aegypti: From natural products to nanoparticles. *Int J Pharm* **2023**, *643*, 123221, doi:10.1016/j.ijpharm.2023.123221.
46. Piombo, E.; Kelbessa, B.G.; Sundararajan, P.; Whisson, S.C.; Vetukuri, R.R.; Dubey, M. RNA silencing proteins and small RNAs in oomycete plant pathogens and biocontrol agents. *Front Microbiol* **2023**, *14*, 1076522, doi:10.3389/fmicb.2023.1076522.

47. Silva, L.E.I.; Paula, A.R.; Ribeiro, A.; Butt, T.M.; Silva, C.P.; Samuels, R.I. A new method of deploying entomopathogenic fungi to control adult Aedes aegypti mosquitoes. *J. Appl. Entomol.* **2018**, *142*, 59-66, doi:10.1111/jen.12402.
48. Bukhari, T.; Takken, W.; Koenraadt, C.J.M. Development of *Metarhizium anisopliae* and *Beauveria bassiana* formulations for control of malaria mosquito larvae. *Parasite Vector* **2011**, *4*, -.
49. Qin, Y.; Liu, X.; Peng, G.; Xia, Y.; Cao, Y. Recent Advancements in Pathogenic Mechanisms, Applications and Strategies for Entomopathogenic Fungi in Mosquito Biocontrol. *J Fungi (Basel)* **2023**, *9*, doi:10.3390/jof9070746.
50. Rodrigues, J.; Bergamini, C.; Montalva, C.; Humber, R.A.; Luz, C. Simple method to detect and to isolate entomopathogenic fungi (Hypocreales) from mosquito larvae. *J. Invertebr. Pathol.* **2021**, *182*, 107581, doi:10.1016/j.jip.2021.107581.
51. Leles, R.N.; Lopez Lastra, C.C.; Garcia, J.J.; Fernandes, E.K.; Luz, C. A simple method for the detection of Leptolegnia chapmanii from infected Aedes aegypti larvae. *Can J Microbiol* **2013**, *59*, 425-429, doi:10.1139/cjm-2012-0703.
52. Accoti, A.; Engdahl, C.S.; Dimopoulos, G. Discovery of Novel Entomopathogenic Fungi for Mosquito-Borne Disease Control. *Front Fungal Biol* **2021**, *2*, 637234, doi:10.3389/ffunb.2021.637234.
53. Kikankie, C.K.; Brooke, B.D.; Knols, B.G.J.; Koekemoer, L.L.; Farenhorst, M.; Hunt, R.H.; Thomas, M.B.; Coetzee, M. The infectivity of the entomopathogenic fungus *Beauveria bassiana* to insecticide-resistant and susceptible *Anopheles arabiensis* mosquitoes at two different temperatures. *Malaria Journal* **2010**, *9*, -.
54. Farenhorst, M.; Knols, B.G.J.; Thomas, M.B.; Howard, A.F.V.; Takken, W.; Rowland, M.; N'Guessan, R. Synergy in efficacy of fungal entomopathogens and permethrin against West African insecticide-resistant *Anopheles gambiae* mosquitoes. *Plos One* **2010**, *5*, -.
55. Farenhorst, M.; Mouatcho, J.C.; Kikankie, C.K.; Brooke, B.D.; Hunt, R.H.; Thomas, M.B.; Koekemoer, L.L.; Knols, B.G.J.; Coetzee, M. Fungal infection counters insecticide resistance in African malaria mosquitoes. *P Natl Acad Sci USA* **2009**, *106*, 17443-17447.
56. Gao, T.N.; Wang, Z.L.; Huang, Y.; Keyhani, N.O.; Huang, Z. Lack of resistance development in *Bemisia tabaci* to I*saria fumosorosea* after multiple generations of selection. *Sci Rep-Uk* **2017**, *7*, doi:ARTN 42727 10.1038/srep42727.
57. Bickel, J.T.; Koehler, A.M. Review of Pythium species causing damping-off in corn. *Plant Health Progress* **2021**, *22*, 219-225.
58. Paul, B.; Bouchet, P.; Bouchet, F. Some species of *Pythium* isolated from soil and water samples collected in western Africa. *Microbiol. Res.* **1994**, *149*, 217-222.
59. Broders, K.D.; Wallhead, M.W.; Austin, G.D.; Lipps, P.E.; Paul, P.A.; Mullen, R.W.; Dorrance, A.E. Association of soil chemical and physical properties with Pythium species diversity, community composition, and disease incidence. *Phytopathology* **2009**, *99*, 957-967, doi:10.1094/PHYTO-99-8-0957.
60. Nam, B.; Choi, Y.J. Phytopythium and Pythium Species (Oomycota) Isolated from Freshwater Environments of Korea. *Mycobiology* **2019**, *47*, 261-272, doi:10.1080/12298093.2019.1625174.
61. Sharma, S.; Sundaresha, S.; Bhardwaj, V. Biotechnological approaches in management of oomycetes diseases. *3 Biotech* **2021**, *11*, 274, doi:10.1007/s13205-021-02810-y.
62. de Andrade Lourenco, D.; Branco, I.; Choupina, A. Phytopathogenic oomycetes: a review focusing on Phytophthora cinnamomi and biotechnological approaches. *Mol. Biol. Rep.* **2020**, *47*, 9179-9188, doi:10.1007/s11033-020-05911-8.
63. Bozkurt, T.O.; Schornack, S.; Banfield, M.J.; Kamoun, S. Oomycetes, effectors, and all that jazz. *Curr. Opin. Plant Biol.* **2012**, *15*, 483-492, doi:10.1016/j.pbi.2012.03.008.
64. Jiang, R.H.; Tyler, B.M. Mechanisms and evolution of virulence in oomycetes. *Annu. Rev. Phytopathol.* **2012**, *50*, 295-318, doi:10.1146/annurev-phyto-081211-172912.
65. Phillips, A.J.; Anderson, V.L.; Robertson, E.J.; Secombes, C.J.; van West, P. New insights into animal pathogenic oomycetes. *Trends Microbiol.* **2008**, *16*, 13-19, doi:10.1016/j.tim.2007.10.013.
66. Gaastra, W.; Lipman, L.J.; De Cock, A.W.; Exel, T.K.; Pegge, R.B.; Scheurwater, J.; Vilela, R.; Mendoza, L. Pythium insidiosum: an overview. *Vet. Microbiol.* **2010**, *146*, 1-16, doi:10.1016/j.vetmic.2010.07.019.
67. Sur, B.; Bihari, V.; Sharma, A.; Joshi, A.K. Studies on physiology, zoospore morphology and entomopathogenic potential of the aquatic oomycete: Lagenidium giganteum. *Mycopathologia* **2002**, *154*, 51-54, doi:10.1023/a:1015273516881.
68. Jaronski, S.; Axtell, R.C. Simplified production system for fungus Lagenidium giganteum for operational mosquito control. *Mosquito News* **1984**, *44*, 377-381.
69. Chen, C.-M.; Hsieh, H.-J.; Hu, B.-Y.; Fu, C.-H. Mosquito-killing water molds isolated from soil samples collected in Taiwan. *Pedobiologia* **2005**, *49*, 585-589.
70. Shen, D.; Wang, J.; Dong, Y.; Zhang, M.; Tang, Z.; Xia, Q.; Nyawira, K.T.; Jing, M.; Dou, D.; Xia, A. The glycoside hydrolase 18 family chitinases are associated with development and virulence in the mosquito pathogen Pythium guiyangense. *Fungal Genet. Biol.* **2020**, *135*, 103290, doi:10.1016/j.fgb.2019.103290.

71. Wang, C.; Shen, D.; Wang, J.; Chen, Y.; Dong, Y.; Tang, Z.; Xia, A. An AGC kinase, PgAGC1 regulates virulence in the entomopathogenic oomycete Pythium guiyangense. *Fungal Biol* **2019**, *123*, 87-93, doi:10.1016/j.funbio.2018.11.006.
72. Sparrow, F.K. Two new species of Pythium parasitic in green algae. *Ann. Bot.* **1931**, *45*, 257-277.
73. Middleton, J.T. The taxonomy, host range, and geographic distribution of the genus Pythium. *Memoirs of the Torrey Botanical Club* **1943**, *20*, 1-171.
74. Poveda, J. *Trichoderma* as biocontrol agent against pests: New uses for a mycoparasite. *Biol. Control* **2021**, *159*, 104634.
75. Chaverri, P.; Castlebury, L.A.; Overton, B.E.; Samuels, G.J. Hypocrea/Trichoderma: species with conidiophore elongations and green conidia. *Mycologia* **2003**, *95*, 1100-1140.
76. Degenkolb, T.; Grafenhan, T.; Berg, A.; Nirenberg, H.I.; Gams, W.; Bruckner, H. Peptaibiomics: Screening for polypeptide antibiotics (peptaibiotics) from plant-protective Trichoderma species. *Chem. Biodivers.* **2006**, *3*, 593-610, doi:10.1002/cbdv.200690063.
77. Lopez-Quintero, C.A.; Atanasova, L.; Franco-Molano, A.E.; Gams, W.; Komon-Zelazowska, M.; Theelen, B.; Muller, W.H.; Boekhout, T.; Druzhinina, I. DNA barcoding survey of Trichoderma diversity in soil and litter of the Colombian lowland Amazonian rainforest reveals Trichoderma strigosellum sp. nov. and other species. *Antonie Van Leeuwenhoek* **2013**, *104*, 657-674, doi:10.1007/s10482-013-9975-4.
78. Amanullah, F.; Khan, W.U. Trichoderma asperellum L. Coupled the Effects of Biochar to Enhance the Growth and Physiology of Contrasting Maize Cultivars under Copper and Nickel Stresses. *Plants (Basel)* **2023**, *12*, doi:10.3390/plants12040958.
79. Chou, H.; Xiao, Y.T.; Tsai, J.N.; Li, T.T.; Wu, H.Y.; Liu, L.D.; Tzeng, D.S.; Chung, C.L. In Vitro and in Planta Evaluation of Trichoderma asperellum TA as a Biocontrol Agent Against Phellinus noxius, the Cause of Brown Root Rot Disease of Trees. *Plant Dis.* **2019**, *103*, 2733-2741, doi:10.1094/PDIS-01-19-0179-RE.
80. Elshahawy, I.E.; Marrez, D.A. Antagonistic activity of Trichoderma asperellum against Fusarium species, chemical profile and their efficacy for management of Fusarium-root rot disease in dry bean. *Pest Manag Sci* **2023**, doi:10.1002/ps.7846.
81. G, R.; Naik, M.K.; Nitnavare, R.B.; Yeshvekar, R.; Bhattacharya, J.; Bhatnagar-Mathur, P.; Sharma, M. Genetic enhancement of Trichoderma asperellum biocontrol potentials and carbendazim tolerance for chickpea dry root rot disease management. *Plos One* **2023**, *18*, e0280064, doi:10.1371/journal.pone.0280064.
82. Herrera-Tellez, V.I.; Cruz-Olmedo, A.K.; Plasencia, J.; Gavilanes-Ruiz, M.; Arce-Cervantes, O.; Hernandez-Leon, S.; Saucedo-Garcia, M. The Protective Effect of Trichoderma asperellum on Tomato Plants against Fusarium oxysporum and Botrytis cinerea Diseases Involves Inhibition of Reactive Oxygen Species Production. *Int J Mol Sci* **2019**, *20*, doi:10.3390/ijms20082007.
83. Batool, R.; Umer, M.J.; Wang, Y.; He, K.; Zhang, T.; Bai, S.; Zhi, Y.; Chen, J.; Wang, Z. Synergistic Effect of Beauveria bassiana and Trichoderma asperellum to Induce Maize (Zea mays L.) Defense against the Asian Corn Borer, Ostrinia furnacalis (Lepidoptera, Crambidae) and Larval Immune Response. *Int J Mol Sci* **2020**, *21*, doi:10.3390/ijms21218215.
84. Saharan, R.; Patil, J.A.; Yadav, S.; Kumar, A.; Goyal, V. The nematicidal potential of novel fungus, Trichoderma asperellum FbMi6 against Meloidogyne incognita. *Sci Rep* **2023**, *13*, 6603, doi:10.1038/s41598-023-33669-z.
85. Podder, D.; Ghosh, S.K. A new application of Trichoderma asperellum as an anopheline larvicide for eco friendly management in medical science. *Sci Rep* **2019**, *9*, 1108, doi:10.1038/s41598-018-37108-2.
86. da Silveira, A.A.; Andrade, J.S.P.; Guissoni, A.C.P.; da Costa, A.C.; de Carvalho, E.S.A.; da Silva, H.G.; Brito, P.; de Souza, G.R.L.; Fernandes, K.F. Larvicidal potential of cell wall degrading enzymes from Trichoderma asperellum against Aedes aegypti (Diptera: Culicidae). *Biotechnol. Prog.* **2021**, *37*, e3182, doi:10.1002/btpr.3182.